Journal of Engineering, Management and Information Technology

ASPUR PUBLISHING

Vol. 04, No. 03 (2026) 257-268, doi:10.61552/JEMIT.2026.03.003 - http://jemit.aspur.rs

DIGITAL RECONSTRUCTION AND CFD-BASED PERFORMANCE MAPPING OF A FRANCIS TURBINE RUNNER USING 3D SCANNING UNDER VARIABLE HEAD AND GUIDE VANE OPENINGS

Irwanda Yuni Pungkiarto
Mohammad Rizanto Juliarsyah [1]
Faradilla Fauziyah Risnawati
Khoirul Anwar
Muhammad Rasyid Ridho

Received 29.11.2025.
Revised 05.02.2026.
Accepted 02.03.2026.

Keywords:

Francis turbine, 3D scanning, reverse engineering, CFD, hydraulic performance, guide vane opening, variable head.

Original research

A B S T R A C T

The performance of Francis turbines in hydropower plants largely depends on the integrity of the runner geometry, which may be affected by wear and tear, cavitation effects, and structural deformation; hence, it requires evaluation with reference to its actual geometry. This research paper aims to address how to accurately reconstruct the runner of a Francis turbine and how to evaluate its hydraulic performance for various heads and vane opening values. The method involves 3D scanning of the runner surface using the structured light method and processing the data to reconstruct the runner geometry using SpaceClaim. The runner geometry is then analyzed for its hydraulic performance using steady-state CFD with the k-ε turbulence model in ANSYS CFX. The runner was simulated for various heads of 44m, 83m, and 122m and for various values of vane opening angles ranging from 1.3 to 19.3 degrees to find discharge, shaft power, and efficiency. The results show that for the given operating head of 83m, the maximum shaft power of 1.275 MW is developed for 19.3 degrees vane opening angle, and the highest efficiency of 91% occurs for 14.3 degrees (BEP). The occurrence of vortices and swirling motions is evident for the runner operating under partial load conditions. Thus, it may be concluded that 3D scanning and CFD are useful tools for runner performance evaluation.

1. INTRODUCTION

Hydropower has been identified as one of the important pillars for the transition to low-carbon electricity generation. The Francis turbine has been found to be one of the most common turbine designs owing to its wide operating range. However, turbine efficiency and stability are largely dependent on runner integrity, which may be affected by cavitation, erosion, and structural deformation under operating conditions. This problem has been further exacerbated by the recent trend of operating hydropower plants under more flexible operating conditions, which requires turbines to operate frequently under off-design conditions (Lee et al., 2025; Mohammadi et al., 2023). Recent research has shown that off-design operation has been linked to flow

[1] Corresponding author: Moh. Rizanto Juliarsyah
Email: Mohammad.rizanto@polinema.ac.id

instability problems, including vortex rope formation and pressure pulsation within the draft tube (Li et al., 2022; Lu & Tao, 2024; Wang et al., 2022; Zainal & Ahmed, 2025).

In order to improve the performance of older turbines, recent digitalization strategies have combined reverse engineering and CFD to reconstruct and evaluate the hydraulic turbine when the original design information is incomplete or unavailable. In particular, the application of inverse design and optimization methods combined with CFD has been identified as one of the viable solutions for turbine refurbishment-oriented redesign and performance recovery (Ohiemi et al., 2025a; Ohiemi et al., 2025b). In addition to this, recent research has shown the applicability of 3D scanning geometry for representing the turbine geometry for the evaluation of erosion effects and geometry-induced performance losses (Narváez et al., 2025; Souček et al., 2024).

In the turbine flow passage, the guide vane opening (GVO) is considered one of the important operational parameters for discharge and incidence. The GVO may drastically change the internal flow structure. In recent studies, it has been found that changing the GVO will change the channel vortex and pressure pulsation of the runner (Hou et al., 2024; Pang et al., 2024). At the same time, the GVO is related to sediment erosion patterns and leakage flow phenomena, which may cause further disturbance to the flow field and deteriorate the turbine performance (Khullar et al., 2024; Song et al., 2022; Sun et al., 2025). The above research results show that it is not appropriate to conduct turbine performance tests by using a single operating condition; rather, it should be tested under multiple operating conditions within the relevant operating heads and GVO (Ji et al., 2022; Lee et al., 2025;).

From the viewpoint of CFD methods, the hydrodynamics of Francis turbines can be analyzed using the RANS equations for steady flows or URANS for unsteady flows. Cavitation modeling can also be used, depending on the type of instability considered. Comparison of results using RANS with those using hybrid RANS-LES methods indicates that the choice of model can significantly affect the simulation of cavitating vortex rope behavior and the associated pressure fluctuations. Analysis of the results of research on the mitigation of the associated instability using design modifications like draft tube design changes, bio-inspired modifications of the guide vanes and/or the draft tube, and the use of stabilizers indicates that the use of CFD is not only for analyzing the problem but also for prescribing the solution to the problem.0

Considering the use of the scan-to-CFD approach in the realm of engineering in Indonesia for the assessment of the hydrodynamic performance of Francis turbine runners in the context of rehabilitation works, it is observed that the approach can be effectively used in the assessment of the hydrodynamic performance of the Francis turbine runners. The use of CFD in the solution of similar fluid dynamics problems related to the aerodynamics of objects in the external flow and the design of small hydro systems indicates the growing capacity of the local engineering community in the use of the CFD approach in the evaluation of the hydrodynamic performance of the Francis turbine runners. However, in most cases, the use of variable head conditions combined with variable GVO conditions in conjunction with flow structure interpretation techniques like pressure contours, vortex lines, and swirl plots, is lacking in most cases in the solution of the associated hydrodynamic problems.

Against the background of the use of the scan-to-CFD approach in the assessment of the hydrodynamic performance of the Francis turbine runner in the context of rehabilitation works in Indonesia, the present study aims to perform a multi-condition assessment of the hydrodynamic performance of the Francis turbine runner that was rebuilt using the reverse engineering approach based on the 3D scan data.

2. LITERATURE REVIEW

2.1. Francis Turbine Performance and Off-Design Operation

Francis turbines are commonly used in hydropower plants due to the efficient performance of the turbine for wide ranges of head and discharges. Nevertheless, the performance of the Francis turbine is highly dependent on the runner's geometry as well as the operating conditions. Current research has also emphasized the importance of the need for the grid, which has increased the chances of the turbine being operated under off-design as well as transient conditions, thus resulting in hydraulic instabilities such as draft tube swirl as well as vortex rope (Arabnejad et al., 2023; Lee et al., 2025; Wang et al., 2022).

2.2. 3D Scanning and Reverse Engineering for "As-Is" Turbine Geometry

In hydropower refurbishment projects, it's common that there's no access to the original design drawings of the turbines, and therefore reverse engineering becomes necessary in order to create the geometries of the turbine according to their actual configuration, or their 'as-is' configuration. 3D scanning technology has been highlighted as a key technology in such processes due to its capability of capturing complex geometries of hydropower turbines with high precision. However, it's common that 3D scanning data are provided with certain levels of noise and missing areas, and may not be properly aligned. In such cases, certain processes are necessary in order to create a valid CAD model suitable for numerical analysis (Liu et al., 2024; Souček et al., 2024; Zhang et al., 2023a). Recent studies on hydropower digitalization have highlighted that it's crucial to maintain realistic geometries of hydropower turbines when analyzing certain components with certain levels of erosion and deformation because such changes may significantly affect the losses of the turbines (Narváez et al., 2025).

2.3. CFD Approaches for Turbine Performance Assessment

Computational Fluid Dynamics (CFD), as an effective means for measuring head, torque, power, efficiency, etc., as well as for developing an accurate picture of the pressure and velocity fields inside hydraulic machines, is the go-to tool for the job. When the objective is the renovation of existing machines, CFD provides an effective paradigm for gauging performance using reconstructed geometries, etc. Recently, research has demonstrated that CFD-based digital methods can be an effective way to revamp existing hydropower plants, improving the operational flexibility of the machines by providing the means for the systematic mapping of the performance of the machines across different operating points (Ohiemi & McNabola, 2025a; Ohiemi & McNabola, 2025b; Walid & Pungkiarto, 2025). Additionally, the integration of global performance metrics with flow field analysis tools, such as pressure contours, streamline analysis, etc., can provide the link between the efficiency characteristics of the machines and the effects of flow separation, secondary flows, etc., that occur during off-design operation (Arabnejad et al., 2023; Wang et al., 2022).

3. METHODOLOGY

The reverse engineering process flowchart is shown in Figure 1. The reverse engineering process of the hydroelectric power plant runner began with 3D scanning data collection of the runner in Figure 4. The 3D scan data became the basis (geometric reference) for 3D runner modeling. The 3D model resulting from the reverse engineering process was verified for hydraulic performance and strength using CFD analysis. 3D modeling was performed using SpaceClaim software, while CFD analysis was performed using ANSYS CFX. 3D modeling is performed using SpaceClaim software, while CFD analysis uses ANSYS CFX (ANSYS, 2025)

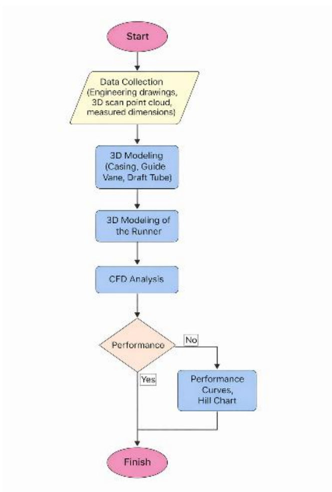

Figure 1. Flow chart of reverse engineering of the Plengan Hydroelectric Power Plant Runner

3.1. 3D Scanning

The 3D scanning process uses a structured light scanner to capture the complex geometry of the runner with high precision. The scanned data in the form of a point cloud is processed using SpaceClaim software to produce a smooth, noise-free mesh. This mesh is then further processed into a solid model in CAD format that can be used for analysis.

3.2. CAD Modeling

The CAD model is created using SpaceClaim software. This process includes converting the mesh into a solid model, smoothing the geometry, and adjusting the dimensions. The resulting CAD model is then used as the basis for CFD simulation. The main objective of 3D modeling is to obtain a 3D runner model that is as close as possible to the actual reference runner in terms of both dimensions and geometry. Thus, the reverse engineering model has the same hydraulic performance characteristics as the actual runner. The 3D modeling process and results are highly dependent on the results of the 3D scanning data acquisition process.

3.3. CFD Simulation

CFD simulation is performed using ANSYS CFX to analyze fluid flow through the runner. The boundary conditions used include flow velocity at the inlet, pressure at the outlet, and runner wall conditions. The k-ε turbulence model is used to describe the flow under operating conditions. The simulation results are analyzed to understand the pressure distribution, fluid velocity, and flow patterns that occur inside the runner.

3.4. CFD simulation process:

3.4.1. Creation of the geometry of the model/problem

The Figure 2 represents the conventional Francis turbine configuration with its spiral casing (pink color), runner with curved blades (blue-green color), and elbow-shaped draft tube (yellow color).

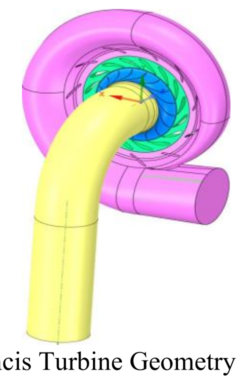

Figure 2. Francis Turbine Geometry Model for CFD Simulation.

The water enters tangentially through the spiral casing and then goes through the blades of the runner and then comes out through the draft tube as shown by the arrow. In conventional turbomachinery theories, the tangential velocity of the runner blades is important for generating torque and is given by the Euler turbine equation (Dixon & Hall, 2014; Wahba, 2022).

The blades of the runner are specially designed to change the direction of the water flow from radial to axial direction. The pressure difference between the pressure side and the suction side of the blades produces a hydrodynamic force to rotate the runner shaft according to the conventional reaction turbine theories (Dixon & Hall, 2014). The above diagram represents the conventional turbine theories with proper guidance of the water flow for efficient conversion of hydraulic energy to mechanical energy.

The elbow-shaped draft tube is specially designed to convert the remaining kinetic energy of the water to pressure energy by gradually increasing the area of the tube. This has been explained by Bernoulli's equation and the law of conservation of energy to enhance the efficiency of the turbine (White, 2016). The recent research has shown that the shape of the draft tube has a significant impact on the formation of the vortex rope and pressure fluctuation under part-load conditions (Lee et al., 2025; Wang et al., 2022). The above diagram represents the conventional Francis turbine theories.

3.4.2. Meshing

he diagram shows the CFD mesh utilized for the analysis of the flow passage through a Francis turbine, consisting of the spiral casing section, the guide vane section, the runner section, and the elbow draft tube section. It is an unstructured mesh with a tetrahedral dominance.

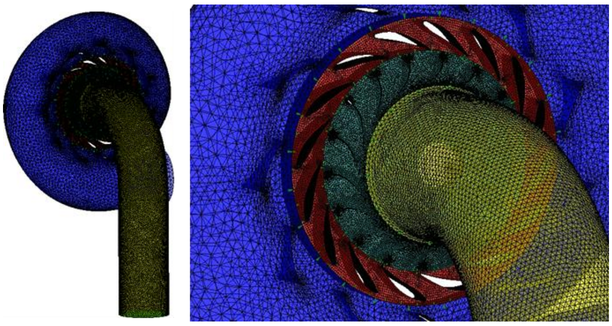

Figure 3. Simulation Domain Meshing

This is a conventional approach to CFD simulation in turbomachinery; the density of the mesh is increased in regions where the flow is highly curved or has a significant amount of turning, separation, or swirling effects (Ferziger et al., 2002; Versteeg & Malalasekera, 2007). While the Figure 3 described the theoretical flow path through a Francis turbine and the energy conversion process, this figure (Figure 3) shows how this process is implemented through a numerical approach. This is a critical aspect of the simulation process since the accuracy of the predicted performance parameters, such as head, torque, efficiency, flow instabilities, such as secondary flows, vortices, and swirling effects in the draft tube section, is highly dependent on the quality and density of the mesh (Dixon & Hall, 2014; Moukalled et al., 2015;). This is a conventional approach to CFD simulation; increasing the density of the mesh around the blades is a good practice since this can reduce numerical diffusion effects in the simulation process, which is a critical aspect according to the conventional approach to the simulation process (Dixon & Hall, 2014).

3.4.3. Definition of physical model

a. k-epsilon turbulence model
b. Fluid = water
c. Density = 998 kg/m3
d. Pressure reference = 1 atm
e. Steady state simulation

3.4.4. Definition of boundary conditions

Throughout the computational domain, the three-dimensional Reynolds-averaged Navier-Stokes equations are solved in conservative form at each mesh element. The k-epsilon model is applied to model turbulent phenomena. Under simulation operating conditions, the mass flow at the spiral inlet and the averaged pressure (0 pa) at the draft tube outlet are used. The simulation was performed at five different guide vane angle openings (1.3º, 4.3º, 9.3, 14.3, 19.3 degrees) at five different head levels (44, 83, 122 meters). The total number of CFD simulations performed was 15. The runner domain was set as a rotating domain with a reference axis rotation of 750 rpm.

3.4.5. The running/solving process, in which the mathematical equations that make up CFD are solved iteratively.

Once the geometry, mesh, physical models, and boundary conditions are defined, the CFD solver starts working on the solution process. It transforms the Reynolds-averaged Navier-Stokes equations, along with the turbulence transport equations, into a set of algebraic equations, which are then solved iteratively. However, the convection terms are highly nonlinear, and the pressure and velocity fields are strongly coupled. Hence, the CFD solver needs to iteratively compute the flow variables until the solution converges.

For example, the CFD solver might prefer coupled solution strategies along with multigrid acceleration techniques to improve the solution reliability and reduce the computational cost, all while maintaining stability for rotating flow problems, as recommended by ANSYS (2025). However, it is recommended that the solution convergence be monitored not just by the residuals, but also by the behavior of the integral parameters, such as the imbalance in the mass flow, torque, head, and efficiency. This is in line with the recent validation work on CFD codes, such as CFX/TurboGrid, where the performance parameters and solution convergence are monitored simultaneously to assess the numerical reliability of the solution, rather than relying on the residuals alone, as recommended by Dickenson et al. (2025).

Moreover, recent literature on CFD solution strategies for turbines highlights the importance of the convergence control, such as the time step, discretization schemes, and turbulence models, which are all essential in the accurate prediction of the swirling, separation, and pressure fluctuation phenomena, which are usually encountered during off-design conditions, as recommended by Abdul Settar et al. (2026).

3.4.6. Analysis and visualization of the CFD solution.
After obtaining the converged solution for the combined problem, we proceed to post-processing to make sense of the physics of the flow and assess how well the turbine performs. This involves extracting global quantities like discharge, hydraulic head, torque, power, and efficiency and using these to construct performance plots and maps. For visualization, we plot pressure and velocity distributions and add streamlines and vortex detection criteria to highlight areas of secondary flows and the development of swirl motions.
In recent years, research articles on turbomachinery and energy-related problems have employed vortex detection criteria like the Q-criterion and its variants to identify areas of vortices associated with pressure fluctuations and instabilities. The general approach has been to combine these criteria with sectionally averaged quantities and monitor points to link these with changes in performance (Shi et al., 2024; Zhou et al., 2024). This same approach has been followed for problems related to cavitation analysis, where vortex visualization criteria are used to make sense of unsteady phenomena responsible for pressure drops and stability issues (Jiang et al., 2025).
To improve confidence in the accuracy of the results obtained via the CFD method, recent articles on verification and validation procedures emphasize the importance of reporting the mesh quality and refinement procedures and estimating the discretization uncertainties using systematic refinement procedures like GCI (Aycan et al., 2023; Gu & Chen, 2024), especially when experimental data are limited.

3.5. Hillchart
A hill chart is a graphical representation used to illustrate the relationship between flow rate (Q), head (H), rotational speed (rpm), runner dimensions (D), and the efficiency of water turbines, particularly Francis turbines. The hill chart displays efficiency contours in the form of hills, where the peaks indicate the optimal conditions for the combination of flow rate, rotational speed, and head that provide the highest efficiency. These contour lines guide turbine users in understanding how changes in flow rate and head affect turbine performance, thereby assisting in adjusting operations so that the turbine operates at maximum efficiency. This is useful for monitoring, optimizing, and planning turbine operations more efficiently. The hill chart for the Francis turbine at the hydroelectric power plant that has been studied is shown in Figure 8. The hill chart calculation formula is shown below.

$$n_{11} = \frac{nD}{\sqrt{H}} \tag{1}$$

$$Q_{11} = \frac{Q}{D^2\sqrt{H}} \tag{2}$$

Where:
n11 = Unit speed value
Q11 = Unit discharge value
n = Rotational speed
D = Runner diameter
H = Turbine head

4. RESULT AND ANALYSYS

4.1. Case Study 1
The scanned 3D model shows the runner geometry in great detail, including the blade profile, shroud, and hub. The resulting mesh has sufficient resolution for further analysis, with minimal errors corrected during data processing. Figure 4 shows the scanned 3D surface mesh, which will be used as a reference when re-modeling the runner.

Figure 4. Runner of a hydroelectric power plant resulting from 3D scanning

The Figure 4 represents the raw 3D scan of the turbine component, which is essentially rendered in a dense form or a point cloud. Although the main structure of the component is well represented, you can see some irregular components or spike-like surfaces, mostly around the lower part of the structure. Such components are quite common in the context of 3D scanning of turbomachinery components in practice, which often appear around occluded areas, very reflective surfaces, or some issues in aligning multiple views or handling outliers during the scanning process. As discussed in the context of reverse engineering theory, the post-processing of the 3D scan is very important before creating a CAD model for CFD analysis (Li, 2021; Sun et al., 2023).
Unlike the above discussion of the Francis turbine flow and energy conversion, which was purely theoretical in nature, the above image represents the upstream stage of the data quality, which is very important for the accurate prediction of runner loading or pressure recovery in the draft tube using CFD analysis. Although the above image represents the raw 3D scan of the turbomachinery component, some components of the 3D model can still be nonphysical in nature, which can cause issues during the CFD analysis of the turbomachinery component. As discussed in recent studies related to reverse engineering of hydraulic turbomachinery components, the

optimization of the point cloud is very important for creating accurate CAD models for CFD analysis (Souček et al., 2024; Walid & Pungkiarto, 2025). As discussed in some studies related to the alignment of the point cloud, the registration of the 3D model is very important when dealing with noisy or outlier-ridden real-world data, which can cause issues in the CAD model due to the accuracy of alignment (Debnath et al., 2025; Denayer et al., 2024).

4.2. Case Study 2

The reference surface model data cannot be directly used as a reference during the 3D model reconstruction process. The data must undergo filtering, removal, and alignment processes to facilitate the reconstruction process and ensure that the reference coordinates are accurate. There are at least three features that must match the reference data during reconstruction, namely the runner, hub, and shroud. Figure 5 shows the 3D model of the hydroelectric power plant runner after remodeling.

Figure 5. 3D model of the Plengan hydroelectric power plant runner after remodeling

The image provided is an illustration of the process from the raw data obtained from the 3D scan to the CAD geometry that is ready for CFD analysis. The left side of the image shows the scanned surface in blue, with many irregularities such as bumps, holes, and other surface defects due to the limited line of sight during scanning, surface reflectivity, and registration noise. Moving to the right side of the image, the surface has now been cleaned up to form a watertight CAD model. This is an indication that the reverse engineering process has taken place to ensure that the runner or casing surface is now ready for meshing or other forms of simulation. This is in line with the new reverse engineering paradigm that the mesh or surface generated from the scanned data is not to be used for CFD analysis, as it may affect the quality of the mesh as well as the pressure distribution results (Liu et al., 2024; Zhang et al., 2023b). Following the earlier discussion regarding the quality of the scanned data in the context of CFD analysis, the image provided is an obvious visual verification that the post-processing stage is where the scanned data is cleaned up to form the CAD geometry that is ready for analysis. The scanning to CAD reconstruction is believed to be an important aspect in the digitalization of hydropower plants for the assessment of refurbishments as well as the development of digital twins for the evaluation of the "as is" conditions (Machalski et al., 2025; Ohiemi & McNabola, 2025a).

4.3. Case Study 3

Table 1 shows the turbine performance parameter values resulting from the CFD simulation. CFD simulation was performed on three guide vane angle conditions, namely 1.3°, 14.3°, and 19.3°, with head variations of 44, 83, and 122 meters. The discharge value in the turbine varies depending on the head and the guide vane angle.

Table 1. Performance of Francis turbines based on simulation results

Guide Vane Angle	*Water Flow*	*Shaft Power*	*Efficiency*
(°)	*(m^3/s)*	*(kW)*	*(-)*
***Head** 44 meter*			
1.3	0.08	0	0
14.3	0.79	223	0.648
19.3	1.07	314	0.674
***Head** 83 meter*			
1.3	0.19	87	0.54
14.3	1.45	1116	0.91
19.3	1.8	1275	0.87
***Head** 122 meter*			
1.3	0.55	187	0.57
14.3	1.84	1945	0.849
19.3	2.42	2189	0.818

At a head of 83 m, which is the actual operating head for the turbine at the hydropower plant, the peak in the power output is achieved when the guide vane is wide open at 19.3°. The peak efficiency of 91% is achieved at a mid-range opening of 14.3°. This indicates that the efficiency peaks at an intermediate opening, which is an indication that the Best Efficiency Point (BEP) is being reached. The results obtained in this research correlate with the results obtained in studies carried out on the performance of Francis turbines. Opening the guide vane increases the discharge, which in most cases increases the power output. However, the efficiency peaks at an intermediate opening as opposed to wide-opening conditions. The efficiency reduces with wide-opening conditions as a result of increased hydraulic losses as well as unfavorable internal flow conditions (Vijay Kumar et al., 2022). When compared with the results obtained in other studies carried out on the performance of Francis turbines, the peak efficiency of 91% is within the range of the efficiency that can be attained in well-performing Francis turbines. The peak efficiency at an intermediate opening instead of a wide-opening condition indicates the "saddle/efficiency drop" that is reached when the Francis turbine is operated at wide-opening conditions instead of the optimal conditions (Krzemianowski & Steller, 2024). Furthermore, recent studies carried out on off-design instabilities indicate that the risk of instability increases as the operating conditions move away from the BEP, especially in the upper part-load as well as the part-load operating regimes (Amini et al., 2023). From the discussions carried out in recent studies carried out in the field of hydropower, it is clear that the use of multi-opening performance curves is essential in the determination of the zones of stability as well as the zones of instability in the performance of the Francis turbine (Figure 6).

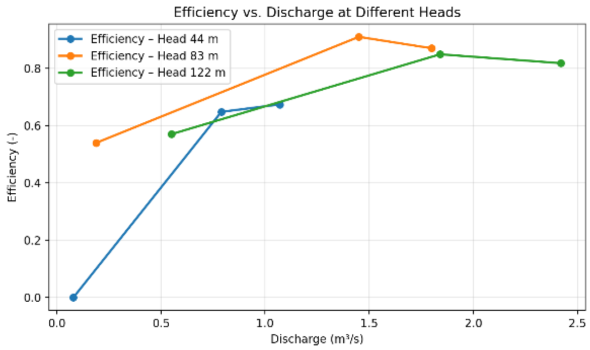

Figure 6. Performance Curve Efficiency vs Discharge

These plots of efficiency against discharge have the standard shape of the Francis turbine curve for different head levels, where the efficiency rises with increasing discharge from its minimum value at low flows, reaches its peak value at some intermediate discharge corresponding to the best efficiency point (BEP), and then gradually falls with increasing discharge. This is in accordance with the recent experimental and numerical studies conducted to investigate hydraulic losses and non-uniformity of flow in the Francis turbines, which have confirmed that such losses are minimized at the BEP, while increasing discharge from this value results in secondary flows and swirl in the draft tube, which can cause erosion of efficiency even at higher discharges (Lee et al., 2025; Mirza Umar et al., 2024). From the results, for the 83 m head case, the maximum efficiency is reached at a discharge of 0.91, while for the 122 m head case, the range of higher efficiencies is wider, but the drop in efficiency at higher discharge is more gentle, indicating additional loss at this condition. Similar results have been obtained in other recent studies of Francis turbines operating away from the BEP, where instabilities in the draft tube and pressure fluctuations are more significant, leading to loss of efficiency (Arabnejad et al., 2023; Lee et al., 2025).

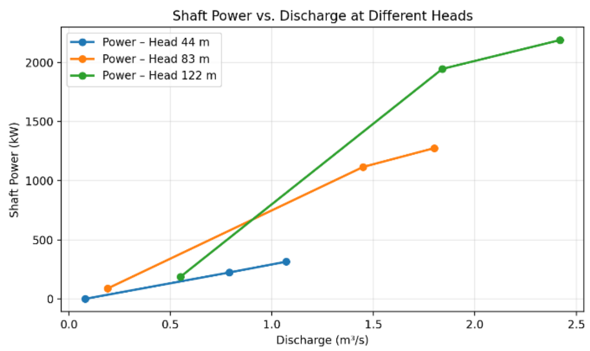

Figure 7. Performance Curve Shaft Power vs Discharge

The curves relating the power and the discharge through the shaft follow a definite and sensible trend for all the head levels (Figure 7). As the discharge increases, the power through the shaft increases in a steady and monotonic fashion. Moreover, the curves themselves lie higher when the head is higher. In other words, when the head is higher, the power through the shaft is higher at the same rate of discharge. This is in complete agreement with the hydraulic power principle, which states that the power is a function of the product of the discharge and the head, apart from the efficiencies. Therefore, when the head or the discharge is increased, the power through the shaft is bound to increase. Such a steady and monotonic increase in the power through the shaft with the increase in the discharge and the opening of the guide vane is also observed in recent studies conducted on Francis turbine machines, where the opening of the vane is increased to increase the flow rate, and in turn, the torque and the power (Vijay Kumar et al., 2022). Similarly, CFD-based studies carried out for the modernization or optimization of Francis turbine machines show the power curves increasing with the discharge, and the improvements or the heads, causing the power to be higher at the same rates of flow. Therefore, the trend in the figure 7 is in complete agreement with the recent assessments and evaluations carried out for the refurbishment and the improvements in the turbine machines (Ohiemi & McNabola, 2025a;).
In general, recent studies and reviews carried out on the off-design operation of the turbine machines state that the operating points and the operating conditions of the turbine machines are primarily a function of the discharge and the head, and the power through the turbine is a function of these two parameters (Lee et al., 2025).

4.4. Case Study 4

The hill chart, Figure 8,plots the efficiency of the turbine for varying values of unit speed n11 and unit discharge Q_{11}.

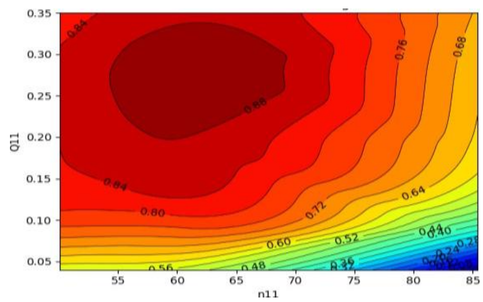

Figure 8. Hill chart of the Francis turbine hydroelectric power plant from the research results

The hill chart represents the region of high efficiency for the turbine. The top of the hill corresponds to the Best Efficiency Point (BEP), which has been identified by recent research on Francis turbines utilizing n_{11} and Q_{11} similarity variables for hill charts to identify the region of stable and high efficiency and to differentiate between the regions of greater hydraulic losses and instability outside the BEP region (Lee et al., 2025; Nam et al., 2025). The hill chart above may be compared with recent research utilizing hill charts for Francis turbines to identify the Best Efficiency Point and to differentiate between the regions of stable and high efficiency and the regions of greater hydraulic losses and instability outside the Best Efficiency Point (Lee et al., 2025; Nam et al., 2025), with the above hill chart being similar to recent research on the rehabilitated Francis turbine utilizing hill charts to identify the Best Efficiency Point and to differentiate between the regions of stable and high efficiency and the regions of greater hydraulic losses and instability outside the Best Efficiency Point (Walid & Pungkiarto, 2025), with the above hill chart being similar to recent research with the familiar single hill structure commonly used as a reference for the selection of efficient and stable operating points (Walid & Pungkiarto, 2025), with contemporary research on characteristic modeling of the Francis turbine further confirming n_{11} and Q_{11} as the standard similarity variables for representing the performance surface of the Francis turbine and for generating efficiency contour maps (Deng et al., 2025a; Deng et al., 2025b).

4.5. Case Study 5

Figure 9-11 shows the water pressure contour on the runner, where the pressure value gradually decreases from the inlet to the outlet of the runner. In the runner, water pressure drops at the outlet because water pressure is converted into mechanical torque work by the runner blades. The figure 9 also shows the pressure difference between the pressure side and suction side of the turbine blades. This pressure difference generates a force on the runner blades, causing torque on the runner shaft.

Guide Vane Angle 1.3°	Guide Vane Angle 14.3°	Guide Vane Angle 19.3°

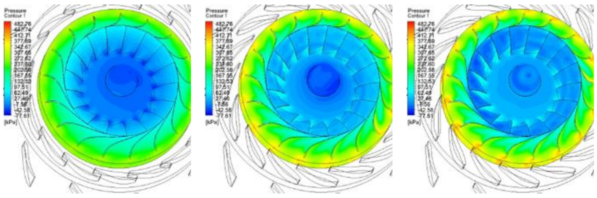

Figure 9. Runner pressure contour at the 44-meter operating head

The figure 9 shows runner pressure contours at a 44 m operating head for three guide vane opening angles (1.3°, 14.3°, and 19.3°).

Guide Vane Angle 1.3°	Guide Vane Angle 14.3°	Guide Vane Angle 19.3°

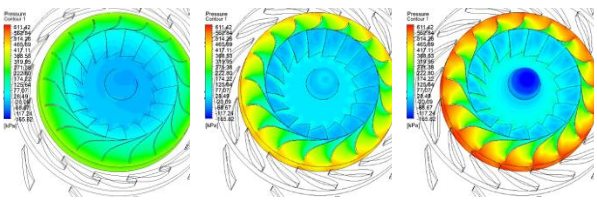

Figure 10. Runner pressure contour at the 83-meter operating head

At 1.3°, the pressure level and blade-to-blade pressure difference are relatively small due to low discharge, indicating low torque. As the opening increases to 14.3° and 19.3°, higher-pressure regions near the runner inlet become more pronounced and the pressure contrast between the pressure and suction sides of the blades increases, which implies higher hydraulic loading and greater shaft power potential.

The figure 10 illustrates the experience of the runner in relation to the pressure contours under an operating head of 83m and guide vane openings of 1.3°, 14.3°, and 19.3°. The small opening of 1.3° has a small pressure and light blade loading, indicating low torque. The opening of 14.3° shows a greater pressure gradient and a greater pressure difference across the blades, indicating a greater hydraulic loading and matching operation in the best-efficiency region. The opening of 19.3° shows a greater extension of high-pressure areas and a greater pressure contrast, indicating a greater blade loading and a greater potential for achieving full power.

Guide Vane Angle 1.3°	Guide Vane Angle 14.3°	Guide Vane Angle 19.3°

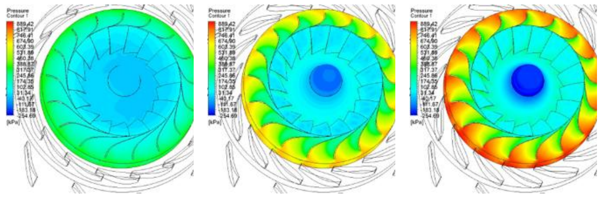

Figure 11. Runner pressure contour at the 122-meter operating head

The figure 11 shows the runner pressure contours for the operating head of 122 m with varying guide vane openings at 1.3°, 14.3°, and 19.3°. When the opening is 1.3°, the pressure field is relatively low and uniform. When the opening is 14.3°, the pressure gradient along the blades is more noticeable. When the opening is 19.3°, the highest pressure areas are near the inlet section and the pressure side of the blades. Therefore, the highest hydraulic loading is attained at this operating condition with the potential for the highest torque and power extraction. This research follows the latest results of the Francis turbine and correlates well with rehab-focused evaluations. It indicates how the shaft power increases with the opening of the vane and the discharge; however, the efficiency remains constant at an intermediate opening and drops off as it goes into off-design operation (Lee et al., 2025; Vijay Kumar et al., 2022). The pressure contours of the runner show how the pressure gradient increases with the opening and the heads; this follows recent CFD results, which show how the opening of the vane has a significant effect on the internal flow structure and pressure field within the runner (Hou et al., 2024; Pang et al., 2024;). Furthermore, the efficiency dropping off as it goes into off-design operation follows recent research regarding how off-design operation has stronger swirl and pressure fluctuations, especially within the draft tube, which increases hydraulic losses and reduces efficiency despite the increase in discharge and power (Lee et al., 2025; Lu & Tao, 2024; Lu et al., 2025). This shows how the scan to CFD workflow provides a useful and practical framework for quantifying the current state of the turbine and provides useful information for maintenance and refurbishment (Ohiemi & McNabola, 2025a; Walid & Pungkiarto, 2025).

4.6. Case Study 6

The fluid flow in the runner and draft tube is shown in Figure 12-14. At the optimum guide vane opening angle where turbine efficiency is highest, the flow in the runner shows the expected flow according to design conditions without flow separation or vortex flow in the runner. At medium openings, only minor secondary flow occurs in the suction side area of the blade near the hub. Flow separation occurs at the small guide vane opening (low flow rate) around the suction side of the blade, marked by vortex flow in the space between the runner blades. This flow also causes local pocket pressure in the space between the blades. The vortex flow phenomenon in the runner will affect the dynamic pressure of the runner. Higher pressure fluctuations also increase the vibration of the runner.

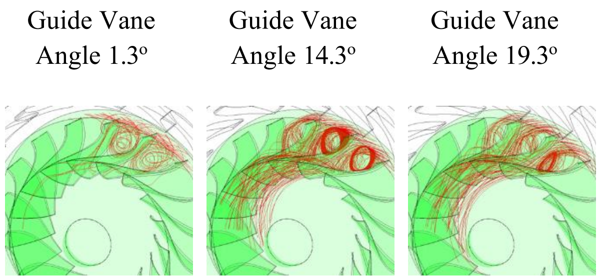

Figure 12. Water flow in the runner at an operating head of 44 meters

The picture shows how the water behaves as it travels through the runner when the operating head is 44 meters, and it considers three openings of the guide vane: 1.3°, 14.3°, and 19.3°. For 1.3°, stronger recirculation and a more defined structure of the vortex are evident within the passages of the blades.

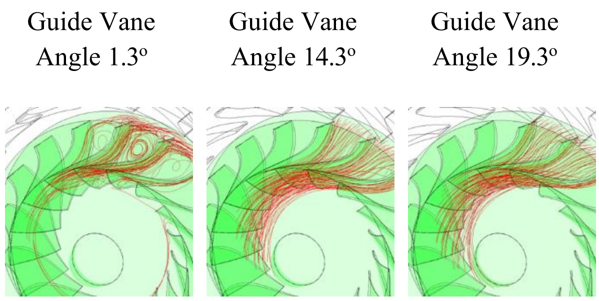

Figure 13. Water flow in the runner at an operating head of 83 meters

This shows the machine operating under partial load conditions with higher losses. For 14.3°, the streamlines are smooth and more uniform, reflecting a more stable condition of the water and better hydraulic performance close to the optimum operating condition. For 19.3°, the water flow remains mostly attached but shows more secondary flow to the outlet of the blades, which may cause additional losses to the machine but not to the optimum.

The figure 13 indicates the nature of flow through the runner at an operating head of 83 m with the guide vane openings at 1.3°, 14.3°, and 19.3°. At an opening of 1.3°, the nature of the streamlines indicates the occurrence of recirculation and vortex flow within the runner blades, indicating instability in the flow process. At an opening of 14.3°, the flow appears to be more uniform with better flow attachment, indicating the most stable condition of flow, which is the most efficient condition. At an opening of 19.3°, the flow is attached except near the outlet.

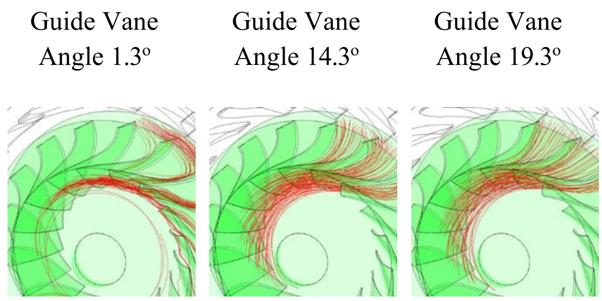

Figure 14. Water flow in the runner at an operating head of 122 meters

The figure 14 depicts the behavior of the flow in the runner at an operating head of 122 m for three different vane openings, namely 1.3°, 14.3°, and 19.3°. At an opening of 1.3°, the streamlines show strong flow non-uniformity with local flow recirculation in the passages, which is characteristic of the partial load operation. At an opening of 14.3°, the flow is smoother and more attached to the blades, which is the most stable state and the best hydraulic performance. At an opening of 19.3°, the flow is more attached, and the streamlines bend more, with stronger secondary flows near the exit. The major conclusion about the fluid flow in the study is that the behavior of the runner is significantly determined by the vane opening and the head. At the smallest vane opening (1.3°), there is a clear indication of recirculation and vortex formation within the blade passages. This is an indication of a part-load operating point, which is usually characterized by higher hydraulic losses. Moving to the next vane opening (14.3°) results in more uniform flow, which is attached to the blade passages. This is an indication of the most stable flow. The flow behavior is consistent with recent studies indicating the effects of the vane opening, which can result in the development of channel vortex and the modification of pressure pulsations within the runner (Pang et al., 2024). At the largest vane opening (19.3°), the flow is still attached, with higher secondary flow and more significant streamline deflection near the blade exit. This is an indication of additional losses, which can be expected at off-design conditions and high discharge operation. The results are consistent with recent studies indicating the effects of off-design conditions, which result in higher instabilities such as swirl and vortex instabilities (Arabnejad et al., 2023; Li, 2024). Unlike the majority of recent studies, which focused on the instability diagnosis within the draft tube or the measurement of pressure pulsation, the results presented in the study can be considered more practical, since they combined the 3D scanning-based reconstruction of the real geometry with the CFD results at different operating conditions. Such an approach is more representative for the refurbishment and "as is" evaluation in real hydropower plants (Hou et al., 2024).

5. DISCUSSION

This study describes how the Francis turbine is expected to behave in normal operating conditions. As the discharge increases and the GVO opens, the power output is expected to increase. However, the maximum efficiency is expected at an intermediate GVO opening, close to the best efficiency point (BEP), and then decreases when the openings become too wide, with increased hydraulic losses (Lee et al., 2025; Pang et al., 2024;). This is in agreement with recent research indicating that operating at conditions far from the BEP may result in flow instability and decreased efficiency, especially in the runner and draft tube configuration (Arabnejad et al., 2023; Wang et al., 2022).
The pressure fields and flow visualizations support the expected behavior. As the head and GVO increase, the pressure gradient and blade force increase, causing the torque and power output to increase. At small GVO openings, the formation of vortices and recirculation is observed, which is consistent with part-load operation. At the BEP, the flow is more likely to be attached and steady, especially in the GVO (Arabnejad et al., 2023; Pang et al., 2024;).

In comparison with previous studies, which may be limited to a specific instability phenomenon or ideal geometry, the results in this study are more applicable to the rehabilitation of the turbine. The geometry used is the "as-is" geometry, which is usually difficult to obtain, and the CFD results at different operating conditions, including head and GVO, make it more applicable to the real-world scenario. This is in agreement with the recent trend in hydropower rehabilitation, which is increasingly adopting CFD for decision support in hydropower rehabilitation (Narváez et al., 2025; Ohiemi & McNabola, 2025a).

6. CONCLUSION

In this study, the Francis turbine runner was successfully remodeled using 3D scanning and analyzed with CFD. Based on the simulation results, at an operating height of 83 meters, a maximum power of 1,275 MW was obtained at a guide vane opening angle of 19.3°, and a maximum efficiency of 91% was achieved at an opening angle of 14.3°. The performance curve illustrates the characteristics of the Francis turbine with the Best Efficiency Point (BEP). Analysis of pressure contours and flow patterns shows pressure gradients on the blades, vortex phenomena, and eddies in the suction pipe under partial discharge conditions. Overall, this method is suitable for assessing and improving runner performance and can be used as a basis for turbine design optimization and maintenance.

Acknowledgement: The authors would like to express their sincere gratitude to the Mechanical Engineering Department, Politeknik Negeri Malang, for providing facilities and technical support during this research. The authors also acknowledge the support from the hydropower plant team for granting access to the turbine runner and operational information required for data acquisition. Special thanks are extended to all colleagues and laboratory staff who contributed to the 3D scanning activities, CAD reconstruction, and CFD simulation processes.

References:

Abdul Settar, N., Sarip, S., & Kaidi, H. M. (2026). Computational Modeling Strategies in Oscillating-Flow Turbine Systems: A Critical Review Based on Wells Turbine Simulations. *Archives of Computational Methods in Engineering*, 1-41.

Amini, A., Vagnoni, E., Favrel, A., Yamaishi, K., Müller, A., & Avellan, F. (2023). Upper part-load instability in a reduced-scale Francis turbine: an experimental study. *Experiments in Fluids*, *64*(6), 110.

ANSYS. (2025). *Ansys CFX-Solver Theory Guide (Release 2025 R1)*. ANSYS, Inc.

Arabnejad, M. H., Nilsson, H., & Bensow, R. E. (2023). Investigation of flow-induced instabilities in a Francis turbine operating in non-cavitating and cavitating part-load conditions. *Fluids*, *8*(2), 61.

Aycan, O., Topuz, A., & Kadem, L. (2023). Evaluating uncertainties in CFD simulations of patient-specific aorta models using Grid Convergence Index method. *Mechanics Research Communications*, *133*, 104188.

Debnath, B., Pourfarash, Z., Ghorpade, B., & Raman, S. (2025). Integrating Reverse Engineering for Digital Model Reconstruction and Remanufacturing of Mechanical Components: A Systematic Review. *Metrology*, *5*(4), 66.

Denayer, M., De Winter, J., Bernardes, E., Vanderborght, B., & Verstraten, T. (2024). Comparison of point cloud registration techniques on scanned physical objects. *Sensors*, *24*(7), 2142.

Deng, X., Hua, H., Li, C., Wei, S., Yan, Z., Deng, W., ... & Liu, X. (2025a). Deformation and stress of a runner in large Francis turbines under wide-load operating conditions. *Water*, *17*(16), 2374.

Deng, Y., Li, Y., Hua, X., Lyu, R., Li, Y., Wang, L., ... & Guo, J. (2025b). A Comprehensive Characteristic Modeling Method for Francis Turbine Based on Image Digitization and RBF Neural Network. *Energies*, *18*(24), 6380.

Dickenson, J., Buick, J. M., Radulovic, J., & Bull, J. (2025). Challenges in CFD Model Validation: A Case Study Approach Using ANSYS CFX and TurboGrid. *Machines*, *13*(7), 593.

Dixon, S. L., & Hall, C. A. (2014). *Fluid mechanics and thermodynamics of turbomachinery* (7th ed.). Butterworth-Heinemann.

Ferziger, J. H., Perić, M., & Street, R. L. (2002). *Computational methods for fluid dynamics* (Vol. 3, pp. 196-200). Berlin: springer.

Gu, H., & Chen, H. C. (2024). Verification and validation of a coupled CFD–FEM approach with overset structured grid through free decay and regular wave tests. *Applied Ocean Research*, *150*, 104126.

Hou, Y., Liu, X., Xiao, M., Zhang, H., Cai, Y., Zeng, Y., ... & Pang, J. (2024). Internal flow characteristics in the draft tube of a Francis turbine under different working conditions. *Advances in Mechanical Engineering*, *16*(10), 16878132241292399.

Ji, L., Xu, L., Peng, Y., Zhao, X., Li, Z., Tang, W., ... & Liu, X. (2022). Experimental and numerical simulation study on the flow characteristics of the draft tube in francis turbine. *Machines*, *10*(4), 230.

Jiang, H. B., Zheng, S. H., Zhang, Y. L., & Guo, H. C. (2025). Applications of different vortex identification methods in cavitation of a self-priming pump. *Scientific Reports*, *15*(1), 7458.

Khullar, S., Tarodiya, R., & Kumar, S. (2024). Study of erosion-induced leakage flow in guide vane of Francis turbine using erosion-coupled mesh deformation simulations. *Powder Technology*, *438*, 119640.

Krzemianowski, Z., & Steller, J. (2024). Basic performance, cavitation and runaway investigations of a high specific speed Francis turbine with emphasis on cavitation analysis: a case study. *Energy Conversion and Management*, *314*, 118653.

Lee, J., Tarannum, S. S., Shrestha, U., Adeeb, E., Ham, S., Kim, S. J., ... & Ha, H. (2025). Francis turbine instabilities during off-design and transient operations: A comprehensive review of the state-of-the-art and recent research and development. *Energy Conversion and Management: X*, 101384.

Li, J., Liu, J., & Chang, W. (2021). CAD Reverse Modeling Based on Multi-sensor Measurement. *Computer-Aided Design & Applications*, *18*.

Li, P., Lu, J., Tao, R., Xiao, R., Ji, B., & Wang, F. (2024). Energy distribution and chaotic pressure pulsation analysis of vortex ropes in Francis-99. *Engineering applications of computational fluid mechanics*, *18*(1), 2310609.

Li, P., Xiao, R., & Tao, R. (2022). Study of vortex rope based on flow energy dissipation and vortex identification. *Renewable Energy*, *198*, 1065-1081.

Liu, Y., Obukhov, A., Wegner, J. D., & Schindler, K. (2024). Point2cad: Reverse engineering cad models from 3d point clouds. In *Proceedings of the IEEE/CVF conference on computer vision and pattern recognition* (pp. 3763-3772).

Lu, J., & Tao, R. (2024). Optimized reduction in draft tube pressure pulsation for a Francis turbine. *Journal of Applied Fluid Mechanics*, *18*(1), 222-240.

Lu, X., Xu, K., Li, T., Xiao, Y., Hu, K., Xu, Y., & Liu, X. (2025). Investigation of Sediment Erosion of the Top Cover in the Francis Turbine Guide Vanes at the Genda Power Station. *Journal of Marine Science and Engineering*, *13*(10), 1923.

Machalski, A., Szulc, P., Błoński, D., Nycz, A., Nemś, M., Skrzypacz, J., ... & Satława, Z. (2025). The concept of a digital twin for the wały śląskie hydroelectric power plant: A case study in Poland. *Energies*, *18*(8), 2021.

Mirza Umar, B., Huang, X., & Wang, Z. (2024). Experimental flow performance investigation of Francis turbines from model to prototype. *Applied Sciences*, *14*(17), 7461.

Mohammadi, M., Hajidavalloo, E., Behbahani-Nejad, M., Mohammadi, M., Alidadi, S., & Mohammadi, A. (2023). Francis turbine draft tube troubleshooting during operational conditions using CFD analysis. *Water*, *15*(15), 2794.

Moukalled, F., Mangani, L., & Darwish, M. (2015). The finite volume method. In *The finite volume method in computational fluid dynamics: An advanced introduction with OpenFOAM® and Matlab* (pp. 103-135). Cham: Springer International Publishing.

Nam, S., Park, J. C., Park, J. B., Yoon, H. K., Terziev, M., & Incecik, A. (2025). Seakeeping analysis of an amphibious vessel using CFD-modified potential (CMP) simulation and experimental validation. *Ocean Engineering*, *328*, 121045.

Narváez, M., Guamán, J., Hidalgo, V. H., Pérez-Sánchez, M., & Ramos, H. M. (2025). Lagrangian Simulation of Sediment Erosion in Francis Turbines Using a Computational Tool in Python Coupled with OpenFOAM. *Machines*, *13*(8), 725.

Ohiemi, I. E., & McNabola, A. (2025a). Supporting the digitalisation of existing hydropower plants using computational fluid dynamics modelling. *Renewable Energy*, 124174.

Ohiemi, I. E., & McNabola, A. (2025b). Design Optimisation of Legacy Francis Turbine Using Inverse Design and CFD: A Case Study of Bérchules Hydropower Plant. *Energies*, *18*(21), 5602.

Pang, J., Yao, B., Liu, X., Li, J., Xiao, M., Jiang, D., ... & Lai, Z. (2024). Influence of guide vane opening on channel vortex and pressure pulsation in Francis turbine runners. *Physics of Fluids*, *36*(4).

Shi, G., Hao, Z., Peng, X., Wen, H., Lv, W., & Fu, J. (2024). Analysis of vortex characteristics in the S-shaped region of a reversible Pump-Turbine with different guide vane openings based on Omega vortex identification method. *Journal of Energy Storage*, *84*, 110921.

Song, X., Zhou, X., Song, H., Deng, J., & Wang, Z. (2022). Study on the effect of the guide vane opening on the band clearance sediment erosion in a Francis turbine. *Journal of Marine Science and Engineering*, *10*(10), 1396.

Souček, J., Bílková, E., & Nowak, P. (2024). Reverse engineering of pump as turbine for CFD analysis. *Acta Polytechnica*, *64*(1), 52-58.

Sun, C., Miao, L., Wang, M., Shi, J., & Ding, J. (2023). Research on point cloud hole filling and 3D reconstruction in reflective area. *Scientific Reports*, *13*(1), 18524.

Sun, L., Wen, M., Sun, S., Xu, Z., & Guo, P. (2025). Numerical investigation of erosion response towards a high-head Francis turbine with special emphasis on clearance sizes effect of guide vane. *Engineering Applications of Computational Fluid Mechanics*, *19*(1), 2565802.

Versteeg, H. K., & Malalasekera, W. (2007). *An introduction to computational fluid dynamics: The finite volume method* (2nd ed.). Pearson.

Vijay Kumar, M., Subba Reddy, T., Sarala, P., Varma, P. S., Chandra Sekhar, O., Babqi, A., ... & Reddy, C. R. (2022). Experimental investigation and performance characteristics of Francis turbine with different guide vane openings in hydro distributed generation power plants. *Energies*, *15*(18), 6798.

Wahba, E. M. (2022). Derivation of the differential continuity equation in an introductory engineering fluid mechanics course. *International Journal of Mechanical Engineering Education*, *50*(2), 538-547.

Walid, A., & Pungkiarto, I. Y. (2025). *Performance study of the Francis turbine runner at Tanggari I hydropower plant via CFD and reverse engineering*. International Journal of Mechanical, Electrical and Civil Engineering, 2(3), 29–45. DOI: 10.61132/ijmecie.v2i3.312

Wang, L., Cui, J., Shu, L., Jiang, D., Xiang, C., Li, L., & Zhou, P. (2022). Research on the vortex rope control techniques in draft tube of Francis turbines. *Energies*, *15*(24), 9280.

White, F. M. (2016). *Fluid mechanics* (8th ed.). McGraw-Hill Education.

Zainal, H. M., & Ahmed, O. K. (2025). Performance assessment of water vortex power plant: Effect of material type and blade number. *Results in Engineering*, *26*, 104775.

Zhang, C., Zhou, H., & Duan, J. A. (2023a). A method for identifying and repairing holes on the surface of unorganized point cloud. *Measurement*, *210*, 112575.

Zhang, T., Hu, Z., Liu, X., Lu, J., Song, X., Zhu, D., & Wang, Z. (2023b). Comparison of Pressure Pulsation Characteristics of Francis Turbine with Different Draft Tube Arrangement Direction. *Water*, *15*(22), 4028.

Zhou, X., Hu, X., Huang, Q., Wu, H., Tang, X., & Cervantes, M. J. (2024). Optimization design of an innovative francis draft tube: Insight into improving operational flexibility. *Energy*, *299*, 131489.

Irwanda Yuni Pungkiarto
State Polytechnic of Malang, Malang, Indonesia (Jl. Soekarno Hatta No. 9, Malang, East Java 65141, Indonesia)
Irwanda.yuni@polinema.ac.id
ORCID: 0009-0001-4669-3311

Mohammad Rizanto Juliarsyah
State Polytechnic of Malang, Malang, Indonesia (Jl. Soekarno Hatta No. 9, Malang, East Java 65141, Indonesia)
Mohammad.rizanto@polinema.ac.id
ORCID: 0009-0004-2630-6582

Faradilla Fauziyah Risnawati
State Polytechnic of Malang, Malang, Indonesia (Jl. Soekarno Hatta No. 9, Malang, East Java 65141, Indonesia)
faradilla.fauziyah@polinema.ac.id
ORCID: 0009-0003-9085-1094

Khoirul Anwar
State Polytechnic of Malang, Malang, Indonesia (Jl. Soekarno Hatta No. 9, Malang, East Java 65141, Indonesia)
khoirul.anwar@polinema.ac.id
ORCID: 0009-0001-3851-8548

Muhammad Rasyid Ridho
State Polytechnic of Malang, Malang, Indonesia (Jl. Soekarno Hatta No. 9, Malang, East Java 65141, Indonesia)
Muhammad.rasyid@polinema.ac.id
ORCID: 0009-0000-6021-7461